Voltage stability in unbalanced power systems: A new complementarity constraints-based approach

Voltage Stability in Unbalanced Power Systems: a new Complementarity Constraints-based approach

Guido Carpinelli
University of Napoli Federico II
Dept. of Electrical Engineering and Information Technology - Napoli, Italy
guido.carpinelli@unina.it

Pierluigi Caramia
University of Napoli Parthenope
Dept. of Engineering
Napoli, Italy
pierluigi.caramia@uniparthenope.it

Angela Russo
Politecnico di Torino,
Energy Department
Torino, Italy,
angela.russo@polito.it

Pietro Varilone
University of Cassino and Southern Lazio
Dept. of Electrical Eng. and Information - Cassino (FR), Italy
varilone@unicas.it

Abstract—Voltage stability has become a fundamental issue in the new, liberalized markets due to the fact that the new power systems are approaching more and more the stability limits. Then, several approaches were proposed in the relevant literature to find the critical conditions and recently the problem was faced also with reference to unbalanced three phase power systems. The unbalances, in fact, can be responsible of more critical stability conditions than in balanced power systems. Continuation power flow and optimal power flows were applied to analyze such conditions. This paper deals with voltage stability analysis in unbalanced power systems and proposes a new optimization model to determine the critical point based on the use of complementarity constraints. Different formulations, with increasing complexity, of the optimization model are proposed and tested. In particular, the maximum stability margin is calculated by a single-stage or a multi-stage procedure that accounts for the relationship between the actual operating point and the maximum loading point. In addition, the multi-stage maximum stability margin problem is formulated also in a probabilistic framework to account for the uncertainties affecting the input data (e.g., load powers). An application is presented on a test system highlighting the feasibility and the goodness of the proposed technique. Both load and line unbalances are taken into account to capture the dependence of voltage stability on the level of unbalances.

Keywords — Power systems, voltage stability, optimization methods, unbalanced systems.

I. INTRODUCTION

In the current framework of competitive electricity markets, the transmission lines' flows are increasing; therefore, power system limits require a deepening also from the new point of view of the open-access scenario and the ability of power systems to meet the load demand has to be carefully examined. In this context, the voltage stability has been recognized as an important issue that System Operators should take into account [1-3, 4].

Voltage stability (VS) refers to the ability of a power system to maintain steady voltages at all buses after a small or large disturbance from a given initial operating condition [2]. This phenomenon can be linked to short-term or long-term problems, leading to "fast" or "slow" variations. VS analysis in power systems has historically concentrated more on the study of operational problems, such as voltage collapse, which can be directly linked to small perturbation phenomena, and thus can be analyzed using steady-state analysis tools, such as power flow-based techniques, as well as linearizations of the system model equations[1] [5].

Several methodologies have been proposed in the relevant literature for steady-state modeling of the voltage stability phenomena in power systems. The main methods appeared to date are based on continuation power flow, modal decomposition and optimization methods [1-3]. The first method reformulates the power flow equations so that they remain well-conditioned at all possible loading conditions. Modal decomposition is based on the analysis of the eigensystem of the reduced Jacobian matrix. The latter methods determine only the critical conditions by solving appropriate optimization problems; these methods are usually more efficient than a continuation power flow method when searching for maximum loading points even though continuation power flows yield intermediate power flow solution information [5].

[1]Generally speaking, the voltage stability phenomenon has been analyzed with both steady-state or dynamic models. Although the dynamic analysis is characterized by a more detailed level of accuracy, the steady-state modeling can be used to analyze effectively many aspects of the voltage stability related to slow dynamic phenomena; moreover, an appropriate static analysis can provide a useful mean to ascertaining the more critical situations to which dynamic analysis can be successively applied [2].

It is worth noting that most of the contributions on voltage stability issues refer to balanced systems. However, not only the distribution systems contain a mixture of single, double and three phase lines and loads but also the transmission systems can be unbalanced due, for instance, to un-transposed lines or single-phase AC traction systems. Recent contributions in the relevant literature have considered power system unbalances in the frame of a continuation three-phase power flow [6] and of optimization methods [7]. Moreover, reference [8] proposed an approach to determine a pair of power-flow solutions associated with the voltage stability of unbalanced three-phase networks; the approach is derived from the observations of the multiple three-phase power-flow solutions of a two-bus network. In [9], the maximum loading point is calculated by applying a first-order polynomial secant predictor and the solution is corrected using the backward/forward radial power-flow method; an adaptive stepwise control is implemented to improve the overall solution process and reduce the number of the calculated points along the traced curve. In the papers addressing voltage stability issues considering power system unbalances, it was clearly demonstrated that the presence of unbalances can generate instability conditions that are more critical than the ones related to balanced power systems.

A key factor of VS analysis of unbalanced power systems is linked to the reactive power limits of generators. In fact, when the power system is highly loaded, the reactive power limits of the generators can be reached and the voltage stability can undergo a deterioration or an immediate voltage collapse can arise [10]. The problem of the generator modeling was faced in unbalanced systems with three-phase continuation power flow [6] and optimization methods [7 - 11].

This paper deals with voltage stability analysis in unbalanced power systems and proposes new optimization models based on the use of complementarity constraints to determine the critical point as initially proposed in [11]. The main features of the optimization model are summarized as follows.

The optimization model allows to evaluate the maximum stability margin of the power system with a three-phase representation of the power systems elements (generators, lines and loads).

The optimization model includes a proper representation of generator busbars that allows the change from PV bus (constant terminal voltage) to PQ bus (constant reactive power) when a generation reactive power limit is reached. This change is obtained including the complementarity constraints in the optimization model; these constraints have been already applied in [3] for balanced systems and here are extended to the unbalanced case. It is worth noting that the variation of typology of busbars during the computational phase was not allowed in the model presented in [7].

Different formulations, with increasing complexity, of the optimization model are proposed and tested in this paper. In particular, the maximum stability margin is calculated by a single-stage or a multi-stage procedure that accounts for the relationship between the actual operating point and the maximum loading point. In addition, the multi-stage maximum stability margin problem is formulated also in a probabilistic framework to account for the uncertainties affecting the input data (e.g., load powers).

The main contributions of this paper are: i) provide a comprehensive optimization model based on the use of complementarity constraints to approach the voltage stability issues for unbalanced systems; ii) formulate a version of the optimization model able to account for uncertainties and to consider more realistic initial operating conditions of the system; iii) provide numerical results with respect to a transmission test system.

It is worth noting that the approach proposed here is substantially different to the one of [11] under different aspects. First, in [11] only a simple single-stage optimization model is considered while this paper proposes different models taking also into account accurately the relationship between the initial operating point and the maximum loading point. Moreover, the model in [11] is formulated only in a deterministic scenario while, in this paper, also the uncertainties of the starting operating point are taken into account. Finally, the numerical applications of this paper are completely different from the ones of [11] because all the proposed optimization models are tested and critically discussed.

The paper is organized as follows. The ability of complementarity constraints to correctly represent the synchronous machine in voltage stability analysis is underlined at first in Section II. The successive section III presents the optimization models including complementarity constraints useful to quantify voltage stability limits in complex unbalanced power systems, with respect to three different formulations. Section IV summarizes simulation results on a test system evidencing the incidence of the generator modeling and line/load-unbalances on the voltage stability limits. In Section V, conclusions are drawn along with future improvements of the research.

II. MODELING OF THE SYNCHRONOUS MACHINE BEHAVIOUR WITH THE COMPLEMENTARY CONSTRAINTS

Voltage collapse is usually associated with load increasing beyond critical limits as well as the lack of reactive power support due to limits in generation or transmission of reactive power [1-3].

In [3] it has been highlighted the great influence of the limited reactive generator capability of synchronous machines on system's behavior with reference to voltage stability. In practice, when the system demand increases, the generator can reach its reactive power limits with the consequence that the generator operation mode changes and the generator modeling should change accordingly from PV (constant terminal voltage) to PQ (constant reactive power) bus modeling.

More in detail, in normal operating conditions the generator operates with constant terminal voltage and with reactive power GQ in the admissible range [GQ_{min} , GQ_{max}]. When the system demand changes starting from a normal operating point, different generator operating modes can arise [3, 12]:

- *Non Limited Mode*: the generator reactive power GQ is between its lower GQ_{min} and upper GQ_{max}values. In this mode the generator terminal voltages is equal to the specified voltage magnitude (the generator bus behaves as a PV bus).
- *Under Excited Mode*: the generator reactive power GQ is at its lower value GQ_{min}, then the generator terminal voltages can be greater than the specified voltage magnitude (the generator bus behaves as a PQ bus).
- *Over Excited Mode*: the generator reactive power GQ is at its upper value GQ_{max}, then the generator terminal voltages can be lower than the specified voltage magnitude (the generator bus behaves once again as a PQ bus).

In practice, the generator that reaches its reactive limit is switched from PV to a PQ bus type.

The above constraints are not immediate to be represented when an optimization approach is applied to solve the voltage stability problem. This is particularly true in case of unbalanced systems where the steady-state generator modeling is much more complex than in balanced conditions. Fortunately, the complementarity constraints can be used to model a change in system behavior.

The complementarity constraint states that the product of two quantities x and y must be zero [12]:

$$x \cdot y = 0. \tag{1}$$

The equation (1) is satisfied if:

$$\begin{aligned} &x = 0 \text{ and } y \neq 0 \\ &y = 0 \text{ and } x \neq 0 \\ &x = 0 \text{ and } y = 0. \end{aligned} \tag{2}$$

The change from a PV to a PQ bus can be modeled by constraint (1) in optimal power flow.

In case of balanced systems, in fact, the following equality constraints are included:

$$\begin{aligned} &(GQ - GQ_{min}) \cdot V_\alpha = 0 \\ &(GQ - GQ_{max}) \cdot V_\beta = 0, \end{aligned} \tag{3}$$

where V_α and V_β are auxiliary *nonnegative* variables that allow increasing or decreasing the generator voltage magnitude V_G respect to the value V_{G0} in normal condition, depending on the value of GQ.

In fact, the voltage generator is expressed as:

$$V_G = V_{G0} + V_\alpha - V_\beta \tag{4}$$

Therefore, the three generator operating mode can be modeled as follow:

if $GQ = GQ_{min} \rightarrow V_\alpha \geq 0$ and $V_\beta = 0 \rightarrow V_G = V_{G0} + V_\alpha$

if $GQ = GQ_{max} \rightarrow V_\alpha = 0$ and $V_\beta \geq 0 \rightarrow V_G = V_{G0} - V_\beta$

if $GQ_{min} < GQ < GQ_{max} \rightarrow V_\alpha = 0$ and $V_\beta = 0 \rightarrow V_G = V_{G0}$.

As is well known, in case of unbalanced systems, the synchronous machine is represented by a 3×3 admittance matrix $\dot{Y}_G$, derived from the sequence component impedances of the machines, which interconnects an internal busbar of balanced three-phase voltages $\overline{E}_G^p$ (p=a, b, c) with a terminal busbar of unbalanced there-phase voltages $\overline{V}_G^p$ (p=a, b, c) (Fig. 1) [12].

The three-phase voltages at terminal busbars, indicated as generator terminal bus voltages, are controlled by the voltage regulator whose behavior must be accurately modeled as it influences the machine operation under unbalanced conditions. The voltage regulator monitors the terminal voltages and controls the excitation voltage according to some predetermined function of the terminal voltages [13]. The "internal bus" voltages $V_{G,i}^p$and "terminal bus" voltages $V_{G,e}^p$ are dependent via the generator admittance matrix; the model is reported in detail in [6].

Often the positive sequence voltage magnitude $V_{G,ps}$ is regulated and it can be extracted from the three-phase voltage measurement using a sequence filter.

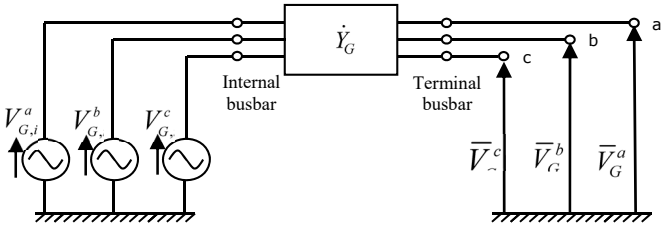

Figure 1 Synchronous machine model

Then, complementarity constraints (3) are yet valid, but with the specification that now V_α and V_β are auxiliary nonnegative variables that allow to increase or decrease the generator positive sequence voltage magnitude in normal operating conditions given by:

$$V_{GO,ps} = \sqrt{\left(V^R_{GO,ps}\right)^2 + \left(V^I_{GO,ps}\right)^2} \tag{5a}$$

with:

$$V^R_{GO,ps} = \frac{Re\left(\bar{V}^a_G + \bar{V}^b_G e^{j2/3\pi} + \bar{V}^c_G e^{j4/3\pi}\right)}{3}$$
$$V^I_{GO,ps} = \frac{Im\left(\bar{V}^a_G + \bar{V}^b_G e^{j2/3\pi} + \bar{V}^c_G e^{j4/3\pi}\right)}{3} \tag{5b}$$

and where $V^R_{GO,ps}(V^I_{GO,ps})$ is the real (imaginary) part of the generator positive sequence voltage in normal operating conditions at the terminal bus and $\bar{V}^p_G$ is the p phase voltage (p = a, b, c) at the generator terminal bus.

Then, eq. (4) becomes:

$$V_{G,ps} = V_{G0,ps} + V_\alpha - V_\beta \tag{6}$$

and the three generator operating mode can be modeled as follow:

if $GQ = GQ_{min} \rightarrow V_\alpha \geq 0$ and $V_\beta = 0 \rightarrow V_{G,ps} = V_{G0,ps} + V_\alpha$

if $GQ = GQ_{max} \rightarrow V_\alpha = 0$ and $V_\beta \geq 0 \rightarrow V_{G,ps} = V_{G0,ps} - V_\beta$

if $GQ_{min} < GQ < GQ_{max} \rightarrow V_\alpha = 0$ and $V_\beta = 0 \rightarrow V_{G,ps} = V_{G0,ps}$.

being GQ the total (three-phase) reactive power, sum of the phase generator reactive powers GQ^p (p = a, b, c); GQ_{min} and GQ_{max} are the lower and upper permissible value for GQ.

III. THREE-PHASE VOLTAGE STABILITY OPTIMIZATION MODELS INCLUDING COMPLEMENTARITY CONSTRAINTS

As evidenced in the previous Section, when the power required by the loads increases from a starting point, the power system approaches the voltage collapse point. A slow varying parameter λ is usually used to represent load changes that move the power system from one equilibrium point to another. This parameter, known as the "loading factor", is introduced in the load power relationships.

In an unbalanced three-phase power system it results[2]:

$$LP^p_k = LP^p_{k,0}(1 + \lambda)$$
$$LQ^p_k = LQ^p_{k,0}(1 + \lambda) \tag{7}$$

where LP^p_k, LQ^p_k are the active and reactive powers at bus k with phase p; and $LP^p_{k,0}, LQ^p_{k,0}$ are their "base" starting power levels.

It should be noted the importance of the base starting power levels $LP^p_{k,0}, LQ^p_{k,0}$ in unbalanced conditions. They characterize the unbalanced nature of the starting loading conditions; for example, a great difference among phase powers introduces a great level of unbalance and the greatest value among the phase powers is associated with the most (critical) loaded phase. Thanks to relationships (7), the same situation happens when the system moves from one equilibrium point to another till the maximum loading conditions.

This section discusses the maximum stability margin problem illustrating the following three different optimization models including complementarity constraints:

A. Single Stage Maximum Stability Margin Model;
B. Multistage Maximum Stability Margin Model;
C. Probabilistic Multistage Maximum Stability Margin Model.

In the following, the three formulations are described in detail.

A. Single Stage Maximum Stability Margin Model

[2] In this paper, for the sake of simplicity, eqs (7) introduce the most simple power changes. More complex relationship can be adopted, e.g. to model a distributed slack bus [3].

This model refers to the traditional steady-state stability problem [12].

The following mixed complementarity problem can be formulated in order to obtain the maximum loading conditions in an unbalanced three-phase power system:

$$\max_{(\boldsymbol{\theta_N},\boldsymbol{V_N},\boldsymbol{V_A},\boldsymbol{GP},\boldsymbol{GQ},\lambda)} \lambda$$

$$\begin{aligned}
\text{s.t.}\quad & F(\boldsymbol{\theta_N},\boldsymbol{V_N},\boldsymbol{V_A},\boldsymbol{GP},\boldsymbol{GQ},\lambda)=0 & \\
& (GQ_j - GQ_{min,j})V_{\alpha,j}=0 & j\in \boldsymbol{\mathcal{G}}\\
& (GQ_j - GQ_{max,j})V_{\beta,j}=0 & j\in \boldsymbol{\mathcal{G}}\\
& V_{j,ps}=V_{j,ps_0}+V_{\alpha,j}-V_{\beta,j} & j\in \boldsymbol{\mathcal{G}}\\
& GQ_{min,j}\le GQ_j\le GQ_{max,j} & j\in \boldsymbol{\mathcal{G}}\\
& GP_{min,j}\le GP_j\le GP_{max,j} & j\in \boldsymbol{\mathcal{G}}\\
& V_{\alpha,j}\ge 0 \qquad V_{\beta,j}\ge 0, & j\in \boldsymbol{\mathcal{G}}
\end{aligned} \tag{8}$$

In the relationships (8):

$\boldsymbol{\theta_N},\boldsymbol{V_N}$	are the vectors of the unknown phase voltage arguments and magnitudes,
$\boldsymbol{V_A}$	is the vector of the auxiliary nonnegative variables,
$\boldsymbol{GP},\boldsymbol{GQ}$	are the vector of the total (three-phase) generator active and reactive powers,
$\boldsymbol{\mathcal{G}}$	is the set of generators except the slack machine,
j	is the generator code
GP_j, GQ_j	are the total j^{th} generator active and reactive powers,
$V_{j,ps}$	is the j^{th} generator positive sequence voltage magnitude,
$GQ_{min,j}, GQ_{max,j}$	are the assigned reactive power limits of the j^{th} generator machine,
$GP_{min,j}, GP_{max,j}$	are the assigned active power limits of the j^{th} generator machine,
V_{j,ps_0}	is the assigned generator positive sequence voltage magnitude in normal conditions,
$V_{\alpha,j}$, $V_{\beta,j}$	are the auxiliary nonnegative variables of the j^{th} generator machine.

It should be noted that the equality constraints $F(\boldsymbol{\theta_N},\boldsymbol{V_N},\boldsymbol{V_A},\boldsymbol{GP},\boldsymbol{GQ},\lambda)=0$ in (8) are the three-phase power flow equations where the active and reactive load powers are expressed by (7). In particular, the three phase load flow model is constituted by the following equations:

- *the active and reactive phase power balance equations at each k^{th} load and generator terminal busbar*:

$$-LP_{k,0}^{p}(1+\lambda)=V_k^p\sum_{i=1}^{N}\sum_{m=a,b,c}V_i^m\left[G_{ki}^{pm}cos\theta_{ki}^{pm}+B_{ki}^{pm}sin\theta_{ki}^{pm}\right]$$

$$-LQ_{k,0}^{p}(1+\lambda)=V_k^p\sum_{i=1}^{N}\sum_{m=a,b,c}V_i^m\left[G_{ki}^{pm}sin\theta_{ki}^{pm}-B_{ki}^{pm}cos\theta_{ki}^{pm}\right]$$

p=a,b,c (9)

where

G_{ki}^{pm}, B_{ki}^{pm}	are the real and the imaginary parts of the terms of the three-phase network admittance matrix relating busbar k with phase p and busbar i with phase m,
V_k^p, θ_k^p	are the voltage magnitude and argument at busbar k with phase p,
$\theta_{ki}^{pm}=$	$\theta_k^p-\theta_i^m$.

- *the voltage equation for the j^{th} generator terminal busbar*:

$$V_{j,ps}=\sqrt{\left(V_{j,ps}^{R}\right)^2+\left(V_{j,ps}^{I}\right)^2} \tag{10}$$

with $V_{j,ps}^{R}$ and $V_{j,ps}^{I}$ given by (6).

The slack machine bus equations depend on the representation adopted. In this paper, without loss of generality, only equation (10) was introduced. Moreover, the angle of the internal voltage of the slack bus is taken as a reference.

- *the total three-phase active and reactive power balance equations at each generator internal busbars except the slack machine.*

These total powers, obtained summing the individual phase active and reactive powers given for each phase, can be related to the magnitudes and angles of the phase voltages via the generator admittance matrix (i.e., $\dot{Y}_G$).

The three-phase voltages at each internal generator busbar are usually assumed to be balanced [6, 13].

More details about the three phase power flow equations can be found in [6,13].

It should be noted that further constraints have to be included, which refer to PV generators. In fact, due to the limitation of the field current, the voltage magnitude at the generator internal bus is limited by the maximum value of the internal voltage of the machine, which corresponds to the maximum field current [6].

It should be also noted that, in the optimization model (8), neither load bus voltage magnitudes limits are considered nor power transfer limits are represented [3]. The reason is why these are considered "hard" limits and not actuation limits, i.e. limits that define undesirable operating conditions which may be associated with system protection rather than system control. Obviously, these limits can be easily included, if of interest.

B. Multistage Maximum Stability Margin Model.

The base operating point strictly affects the voltage stability of the system and, in particular, the maximum loading point that can be determined by solving the optimization problem (8). An accurate determination of the base operating point can allow to obtain more significant results of the maximum stability margin problem.

The multistage maximum stability margin model allows to accurately describe the link between the base, or current, operating point and the maximum loading point [12]. It consists of two steps.

In the first step, the starting operating point is calculated and passed into the second step. In the second step, the maximum stability problem is solved, starting from the "base operating point" calculated in the first step.

In the following, the two steps are illustrated in detail.

Step i.) This step is devoted to the determination of the steady state system operating conditions that is the "base operating point". The load powers ($LP_{k,0}^{p}, LQ_{k,0}^{p}$, for each busbar k and for p=a, b, c) are assigned and the control variables at the generator busbars are calculated. In particular, the values for the positive sequence voltage magnitude at the generator busbars (V_{j,ps_0} for each generator $j \in \mathcal{G}$) are determined.

There are several ways to obtain the base operating point and, then, the values for the control variables at the generator busbars that are inputs of the next step.

In this paper, an Optimal Power Flow (OPF) problem is applied, as an example, to determine the base operating point of the system that corresponds to the minimum system power losses.

The following OPF problem is formulated:

$$\begin{aligned} \min_{(\boldsymbol{\theta_N}, \boldsymbol{V_N}, \boldsymbol{GP}, \boldsymbol{GQ})} \; & P_{loss} \\ \text{s.t.} \quad & F(\boldsymbol{\theta_N}, \boldsymbol{V_N}, \boldsymbol{GP}, \boldsymbol{GQ}) = 0 \\ & GP_{min,j} \le GP_j \le GP_{max,j} \qquad j \in \mathcal{G} \\ & GQ_{min,j} \le GQ_j \le GQ_{max,j} \qquad j \in \mathcal{G} \\ & V_{min,j} \le V_{j,ps\_0} \le V_{max,j} \qquad j \in \mathcal{G} \\ & V_{min,k} \le V_k^p \le V_{max,k} \qquad k \in \mathcal{L} \; p=1,2,3 \end{aligned} \tag{11}$$

In (11) P_{loss} are the system power losses; $V_{min,j}$ and $V_{max,j}$ are lower and upper bounds for the positive sequence voltage magnitude for the j^{th} generator; V_k^p is the phase voltage magnitude at phase p of the k^{th} load busbar ; $V_{min,k}$ and $V_{max,k}$ are lower and upper bounds for the phase voltage magnitude at load busbar k; $\mathcal{L}$ is the set of the load buses.

The equality constraints $F(\boldsymbol{\theta_N}, \boldsymbol{V_N}, \boldsymbol{GP}, \boldsymbol{GQ}) = 0$ in (11) are again the three-phase power flow equations.

Step ii.) The maximum stability problem is solved starting from the "base operating point" determined at the first step.

In this step a mixed complementarity problem such as the Single Stage Maximum Stability Margin Problem (relationships (8)) is solved using the pre-fixed load conditions (i.e., $LP_{k,0}^{p}, LQ_{k,0}^{p}$) and the results from the first step (i.e., value of the positive sequence voltage V_{j,ps_0}).

It should be noted that any other procedure may be used at the first step to calculate the base operating point and not necessarily an optimization problem. Moreover, other limits can be included in both first and second step, if considered adequate.

It should be also noted that the voltage at generator busbars are the same in both conditions (base operating point and maximum loading point) only if the generator reactive limits are not reached approaching the voltage instability. When the limits are reached, the generator voltage at the maximum loading point are allowed to change accordingly.

C. *Probabilistic Multistage Maximum Stability Margin Problem*.

The formulation previously described assumes that the calculation of the base operating point is effected assuming the load conditions known with certainty and assigned as input data (for example, for the OPF (11)).

In real cases, the load powers of an electrical system may be affected by uncertainties; hence, a probabilistic formulation has to be adopted [14-17] .

In this paper, a probabilistic approach to account for uncertainties in voltage stability problem is proposed. This approach is able to take into account the influence of the randomness of initial load conditions on the voltage collapse point.

In the new proposed Probabilistic Multistage Maximum Stability Margin Problem, the two steps are conducted using the probabilistic approach shown in Figure 2.

From the knowledge of the probability density function (pdf) of the active and reactive load phase powers, the pdf of the positive sequence of the voltage magnitude at generator terminal busbars are obtained applying the probabilistic OPF (*step i*).

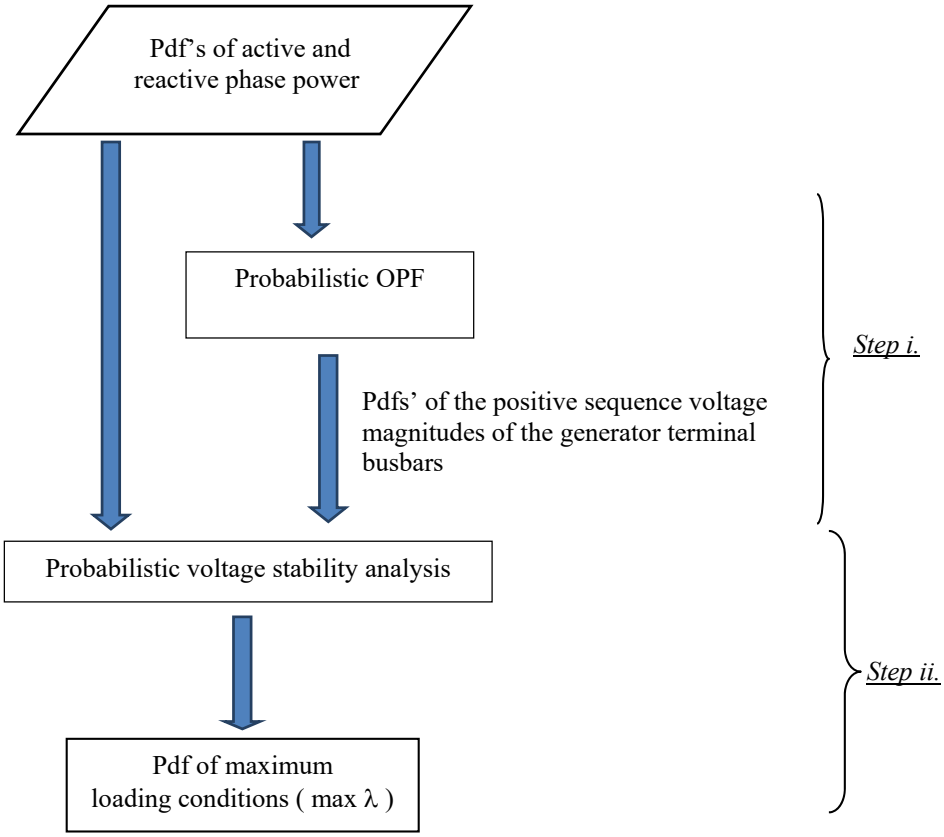

Figure 2 - Flow chart of the Probabilistic Multistage Maximum Stability Margin Problem

Using the pdf calculated at *step i* and the pdf of the active and reactive phase powers, that statistically characterize the base operating points, a probabilistic voltage stability problem is solved to obtain the pdf of the maximum loading conditions (*step ii*).

In this paper a Monte Carlo simulation procedure is applied to perform the probabilistic optimal power flow analysis of an unbalanced three phase power system. Applying this procedure, a value of each random input variable (i.e. the active and reactive phase load powers) is generated according to its proper pdf. Using the generated input values, the optimization problem (11), modeling the OPF problem of the three-phase unbalanced power system, is solved and the values of the positive sequence of the voltage magnitude at generator terminal busbars are obtained.

In practice, for each generated value of the phase active and reactive load powers, in the first step of procedure, a base operating point is calculated.

Starting from the calculated base operating point, the second step is applied to obtain the maximum loading conditions. The second step consists of solving, for each set of values of random input variables (active and reactive phase load powers, positive sequence of voltage magnitude at generator busbar), the mixed complementarity problem whose formulation is given by (8).

This procedure is repeated a sufficient number of times in order to obtain a good estimate of the probability of the output variables according to the stated accuracy.

IV. NUMERICAL APPLICATIONS

The voltage stability optimization model including complementarity constraints illustrated in Section III has been applied to evaluate the stability limits of the three phase transmission test system shown in Fig. 3 [17]. Tables I-IV show the load starting values $LP_{k,b}^{p}, LQ_{k,b}^{p}$ in balanced conditions and the component parameters (in per unit on a 33.33 MVA base). The load starting values at buses #4, #5, #6 and #7 are zero at all phases. The bus #7 is the slack and it is modelled as a constant voltage bus with its angle assumed as the reference.

The algorithm applied to solve the optimization problem is based on the Sequential Quadratic Programming method available in MATLAB® Optimization Toolbox.

The stability analysis has been conducted both for a balanced and an unbalanced three phase power system obtained introducing line and load unbalances in the test system of Fig. 3.

In particular, the three formulations presented in the Section III (Single Stage Maximum Stability Margin Problem, Multistage Maximum Stability Margin Problem and Probabilistic Multistage Maximum Stability Margin Problem) have been applied.

Therefore for each formulation two case studies have been performed by maximizing the loading factor λ; in particular:

Case 1: the loading factor λ is maximized considering symmetrical structure and balanced loads.

Case 2: the loading factor λ is maximized substituting the balanced line 1-2 with an unbalanced line whose series-impedance and shunt-admittance matrices are given in Tables V and VI and introducing unbalanced loads given by:

$$\begin{aligned}
LP_k^a &= LP_{k,0}^a\,(1+\lambda) = 1.1\,LP_{k,b}^a\,(1+\lambda)\\
LP_k^b &= LP_{k,0}^b\,(1+\lambda) = 0.9\,LP_{k,b}^b\,(1+\lambda)\\
LP_k^c &= LP_{k,0}^c\,(1+\lambda) = 1.0LP_{k,b}^c\,(1+\lambda)\\
LQ_k^a &= LQ_{k,0}^a\,(1+\lambda) = 1.1\,LQ_{k,b}^a(1+\lambda)\\
LQ_k^b &= LQ_{k,0}^b\,(1+\lambda) = 0.9\,LQ_{k,b}^b(1+\lambda)\\
LQ_k^c &= LQ_{k,0}^c\,(1+\lambda) = 1.0LQ_{k,b}^c\,(1+\lambda) \qquad \text{with } k=1,2,3
\end{aligned} \tag{12}$$

In practice, in Case 2 the loading factor λ is maximized considering dissymmetrical structure and unbalanced loads.

Case 3: As Case 2 with the base operating point calculated applying the minimization of the total production costs.

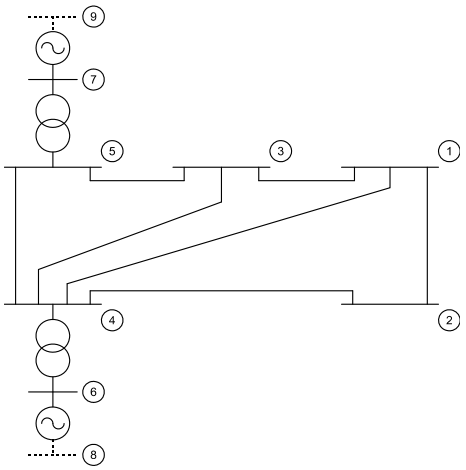

Figure 3 – Test system

TABLE I - BASE ACTIVE AND REACTIVE PHASE LOAD POWERS IN BALANCED CONDITIONS

Bus Code k	**Phase code P**	**Active power $LP^{p}_{k,b}$ [p.u.]**	**Reactive power $LQ^{p}_{k,b}$ [p.u.]**
1	a, b and c	0.40	0.05
2	a, b and c	0.60	0.10
3	a, b and c	0.45	0.15

TABLE II - GENERATOR PARAMETERS

Starting and ending busbars	**Reactances**		
	Positive sequence [p.u.]	**Negative sequence [p.u.]**	**Zero sequence [p.u.]**
6 – 8	0.86	0.22	0.109
7 – 9	0.86	0.22	0.109

TABLE III - TRANSFORMER PARAMETERS

Starting and ending busbars	**Reactance [p.u.]**
4 – 6	0.10
5 – 7	0.10

TABLE IV - LINE PARAMETERS

Starting and ending busbars	**Impedance**					
	Positive and negative sequence			**Zero sequence**		
	Resistance [p.u.]	**Reactance [p.u.]**	**Susceptance [p.u.]**	**Resistance [p.u.]**	**Reactance [p.u.]**	**Susceptance [p.u.]**
1 - 3	0.01	0.03	0.02	0.03	0.09	0.012
3 - 5	0.08	0.24	0.05	0.24	0.72	0.030

4 - 5	0.02	0.06	0.06	0.06	0.18	0.036
3 - 4	0.06	0.18	0.04	0.18	0.54	0.024
1 - 4	0.06	0.18	0.04	0.18	0.54	0.024
2 - 4	0.04	0.12	0.03	0.12	0.36	0.018
1 - 2	0.08	0.24	0.05	0.24	0.72	0.030

TABLE V - SERIES IMPEDANCE MATRIX OF THE UNBALANCED LINE FROM BUS 1 TO 2 [p.u.]

0.0066+j0.056	0.0017+j0.027	0.0012+j0.021
0.0017+j0.027	0.0045+j0.0047	0.0014+j0.022
0.0012+j0.021	0.0014+j0.022	0.0062+j0.061

TABLE VI - SHUNT SUSCEPTANCE MATRIX OF THE UNBALANCED LINE FROM BUS 1 TO 2 [p.u.]

0.150	-0.030	-0.010
-0.030	0.250	-0.020
-0.010	-0.020	0.125

Formulation A: Single Stage Maximum Stability Margin Problem

The generator positive sequence voltage magnitudes are fixed to 1.07 p.u. and 1.08 p.u. at bus #6 and #7, respectively. With reference to the admissible power range of the generator at bus #6, the range [$GQ_{min,6}$ = *-1,* $GQ_{max,6}$ = *+1*] p.u. for reactive power and the range [$GP_{min,6}$ = *0,* $GP_{max,6}$ = *+4*] p.u. for active power are assumed.

Table VII shows the loading factor values at the voltage collapse point (λ_{max}) for both cases.

The analysis of Table VII clearly reveals that the unbalanced loads and dissymmetrical structure can significantly affect the system loading capability, as shown theoretically in [7] and by simulations in [6, 7]. In this case we have a reduction of λ_{max} of about 27,4%.

In both cases, the total generator reactive power reaches its upper value before the critical point, and then the value of the generator positive sequence voltage magnitude at bus #6 at the critical point is different from the specified voltage magnitude in normal conditions (i.e., 1.07 p.u.); in particular, the generator positive sequence voltage magnitude at the critical point is $V_{6,ps}$ = 0.845 p.u for case study 1 and = 1.017 p.u. for case study 2.

In case 2, the voltage amplitudes of the three different phases are significantly unbalanced at the collapse point. Table VIII reports the phase voltage amplitudes at collapse point at all load busbars obtained in this case. It is interesting to observe that, as foreseeable, the voltages at phase a are characterized by the lowest amplitudes being this phase the most loaded one (see (12)).

TABLE VII - LOADING FACTOR VALUES AT CRITICAL POINT – *FORMULATION A*

Case study		**Maximum loading factor (λ_{max})**
Case 1:	Symmetrical structure and balanced loads	1.083
Case 2:	Unsymmetrical structure and unbalanced loads	0.786

TABLE VIII - VOLTAGE AMPLITUDES AT CRITICAL POINT IN THE PRESENCE OF DISSYMMETRICAL STRUCTURE AND UNBALANCED LOADS (CASE 2) – *FORMULATION A*

Load Bus	**Voltage Amplitude [pu]**		
	Phase a	**Phase b**	**Phase c**
#1	0.7585	1.0513	1.0046
#2	0.7549	1.0540	1.0022
#3	0.7633	1.0470	1.0077

#4	0.8791	1.0430	1.0582
#5	0.9308	1.0596	1.0887

As expected, the load unbalances have a significant influence on the voltage stability conditions. Therefore, in order to better evidence the influence of the load unbalances, Table IX shows the value of the loading factors at critical point obtained by varying the load conditions.

In particular, the values reported in Table IX were calculated in the:

- **Case 2.a**: presence of a greater load unbalance:

$$LP_k^a = LP_{k,0}^a\,(1+\lambda) = 1.15\,LP_{k,b}^a\,(1+\lambda)$$
$$LP_k^b = LP_{k,0}^b\,(1+\lambda) = 0.85\,LP_{k,b}^b\,(1+\lambda)$$
$$LP_k^c = LP_{k,0}^c\,(1+\lambda) = 1.0LP_{k,b}^c\,(1+\lambda)$$
$$LQ_k^a = LQ_{k,0}^a\,(1+\lambda) = 1.15\,LQ_{k,b}^a(1+\lambda)$$
$$LQ_k^b = LQ_{k,0}^b\,(1+\lambda) = 0.85\,LQ_{k,b}^b(1+\lambda)$$
$$LQ_k^c = LQ_{k,0}^c\,(1+\lambda) = 1.0LQ_{k,b}^c\,(1+\lambda)$$

with k=1,2,3

Case 2.b: presence of a lower load unbalance:

$$LP_k^a = LP_{k,0}^a\,(1+\lambda) = 1.05\,LP_{k,b}^a\,(1+\lambda)$$
$$LP_k^{2b} = LP_{k,0}^b\,(1+\lambda) = 0.95\,LP_{k,b}^b\,(1+\lambda)$$
$$LP_k^c = LP_{k,0}^c\,(1+\lambda) = 1.00\,LP_{k,b}^c\,(1+\lambda)$$
$$LQ_k^a = LQ_{k,0}^a\,(1+\lambda) = 1.05\,LQ_{k,b}^a(1+\lambda)$$
$$LQ_k^b = LQ_{k,0}^b\,(1+\lambda) = 0.95\,LQ_{k,b}^b(1+\lambda)$$
$$LQ_k^c = LQ_{k,0}^c\,(1+\lambda) = 1.00\,LQ_{k,b}^c\,(1+\lambda)$$

with k=1,2,3

From the results reported in Table IX, it is evident that, in the analyzed cases, the variation of the base load unbalances significantly influences the value of the loading factor at critical point.

In particular, as foreseeable, an increase of the load unbalance, causing an increase of the power in the most loaded phase, that is phase a , from $1.1\,LP_{k,b}^a\,(1+\lambda)$ to $1.15\,LP_{k,b}^a\,(1+\lambda)$, produces the attainment of the critical point with a smaller value of λ ($\lambda_{\text{max\_Case 2.a}} = 0.686$ versus $\lambda_{\text{max\_Case 2}} = 0.786$). On the contrary, a decrease of the load unbalance, that decreases the load at phase a from $1.1\,LP_{k,b}^a\,(1+\lambda)$ to $1.05\,LP_{k,b}^a\,(1+\lambda)$, produces the attainment of the critical point with a larger value of λ ($\lambda_{\text{max\_Case 2.b}} = 0.906$ versus $\lambda_{\text{max–Case 2}} = 0.786$).

TABLE IX - LOADING FACTOR VALUES AT CRITICAL POINT - *FORMULATION A*

Case study		**Maximum loading factor (λ_{max})**
Case 2.a	load unbalance equal to 15% and dissymmetrical structure	0.686
Case 2.b	load unbalance equal to 5% and dissymmetrical structure	0.906

Formulation B: Multistage Maximum Stability Margin Problem.

In the multistage procedure, the OPF model expressed by (11) is solved at the first step.

The lower and upper bounds for generator active and reactive powers and for the generator positive sequence voltage magnitude fixed at busbar #6 in the OPF model are reported in Table X. For the load busbars, the phase voltage magnitude is constrained between 0.9 and 1.1. p.u.

The results of the OPF represent the base operating point, expressed by the starting values of positive sequence of voltage magnitude at the generator terminal busbars #6 and at slack bus #7. Table XI reports the values of these quantities obtained by minimizing the power system losses (i.e., optimization problem (11)).

We note that the regulated voltage at generator busbars, in Case 1, are equal to the maximum permissible value (1.1 p.u.) since the objective function of the OPF model is the minimization of the system power losses. In Case study 2, the positive sequence of the voltage amplitude at the generator busbars do not achieve the maximum value, as it happens in Case study 1, because the constraint on the maximum phase voltage amplitude at phase b of the load busbar #4 is binding.

TABLE X - LOWER AND UPPER BOUNDS OF GENERATORS - *FORMULATION B*

Bus	**Active power [p.u.]**		**Reactive power [p.u.]**		**Positive sequence voltage amplitude [p.u.]**	
	GP_{min}	GP_{max}	GQ_{min}	GQ_{max}	V_{min}	V_{max}
#6	0	4	-1	1	0.9	1.1

TABLE XI - POSITIVE SEQUENCE VOLTAGE MAGNITUDE AT GENERATOR BUSBARS (BASE OPERATING POINT) - *FORMULATION B*

Case study	**Positive sequence voltage amplitude [p.u.]**	
	Bus #6	Bus #7
Case 1	1.100	1.100
Case 2	1.080	1.076

The calculated positive sequence voltage magnitude at the generator terminal busbars, together with the assigned active and reactive phase load powers, define the base operating point used in the voltage stability analysis to be carried out in the second step of the multistage procedure.

Table XII shows the loading factor values at the voltage collapse point for both cases.

The analysis of Table XII clearly reveals that, analogously to the results obtained applying the Formulation A, the unbalanced loads and dissymmetrical structure significantly affect the system loading capability, causing a reduction of λ_{max} of about 32.5%.

Comparing the values of Tables VII and Table XII, it is interesting to note that the Formulation B furnishes maximum loading factor values greater than the Formulation A does in Case 1 (symmetrical structure and balanced load), but an opposite behavior can be observed in Case 2 (dissymmetrical structure and unbalanced load).

The results obtained with two formulations, being the law of the load power variation coincident, are different because the voltage regulation at generator busbars is different; this confirms that the starting operating point influences the stability limit of the network.

The total reactive power generated at bus #6 reaches its upper value before the critical point, and then the generator positive sequence voltage magnitude at bus #6 assumes a value, at the critical point, lower than the specified voltage magnitude in starting operating condition. This happens in both cases; in fact, the generator positive sequence voltage magnitudes at the critical point are, respectively, $V_{6,ps}$ =0.861 p.u. for Case 1 and $V_{6,ps}$ =1.014 p.u. for Case 2.

In the case study 2, the voltage amplitudes of the three different phases are significantly unbalanced at the collapse point, as reported in Table XIII. As foreseeable, the voltages at phase a are characterized by the lowest values of amplitude being this phase the most loaded one.

TABLE XII - LOADING FACTOR VALUES AT CRITICAL POINT – *FORMULATION B*

Case study		**Maximum loading factor (λ_{max})**
Case 1:	Symmetrical structure and balanced loads	1.146
Case 2:	Unsymmetrical structure and unbalanced loads	0.774

TABLE XIII - VOLTAGE AMPLITUDES AT CRITICAL POINT IN THE PRESENCE OF DISSYMMETRICAL STRUCTURE AND UNBALANCED LOADS (CASE 2) – *FORMULATION B*

Load Bus	**Voltage Amplitude [pu]**

	Phase a	Phase b	Phase c
#1	0.756	1.048	1.001
#2	0.752	1.050	0.999
#3	0.760	1.043	1.004
#4	0.876	1.039	1.055
#5	0.926	1.056	1.085

Formulation C: Probabilistic Multistage Maximum Stability Margin Problem.

A Monte Carlo simulation procedure was applied to perform the Probabilistic Multistage Maximum Stability Margin Problem.

As already illustrated in Section III, the step *i* and *ii* are repeated a sufficient number of times (10.000 trials) to obtain a good estimate of the output pdf's according to stated accuracy.

With reference to the statistical characterization of the random input variables, the phase load powers are characterized by uncorrelated Gaussian pdfs. In particular:

- in Case 1, the active and reactive phase load powers are equal on the three phases and characterized by mean values reported in Table I; the standard deviations are equal to 10% of the mean values;
- in Case 2, the active and reactive phase load powers are characterized by mean values calculated using relationships (12); the standard deviations are equal to 10% of the mean values.

The main results obtained in the two cases are illustrated in the following.

Case 1

The lower and upper bounds for generators active and reactive power and for the generator positive sequence voltage magnitude imposed in the OPF model are the same considered in the *Multistage Maximum Stability Margin Problem* (see Table X).

As an example of the results obtainable at the end of the first step, Table XIV reports the mean values and the standard deviations of the positive sequence voltage magnitude at the generator terminal busbars #6. The mean values are practically coincident with the ones obtained applying the step *i* of the *Multistage Maximum Stability Margin Problem* (Table XI).

The pdf's of the voltage magnitude at the generator terminal busbar, output of the first step, together with the pdf of the active and reactive phase load powers (that are the random input data) permit to statistically characterize the base operating point used in the voltage stability analysis performed at the second step of the multistage procedure.

Also in the application of the probabilistic formulation, the voltage stability analysis has been conducted considering the range [$GQ_{min,6} = -1$, $GQ_{max,6} = +1$] p.u. as admissible reactive power range and the range [$GP_{min,6} = 0$, $GQ_{max,6} = +4$] p.u. as admissible active power range. The total reactive power of the generator at busbar #6 reaches its upper value before the critical point for the vast majority of trials and, consequently, the value of the positive sequence voltage magnitude at the critical point is lower than the specified voltage magnitude at the base operating point. In fact, the mean value of the positive sequence voltage magnitude at bus #6 results to be 0.860 p.u. lower than the mean value of 1.1 p.u. of the base operating point; this value practically coincides with the value obtained in Case 1 - Formulation B (0.861 p.u.).

Table XV reports the mean values and the standard deviations of the loading factor at the voltage collapse point. Once again, we can observe that the mean value of the maximum loading factor is practically coincident with the one obtained with the Formulation B.

Eventually, as an example of the obtainable results, Fig. 4 shows the pdf of the maximum loading factor; from the graph, we can observe that the shape of the pdf approaches a Gaussian pdf .

Table XVI reports the mean value of the phase voltage amplitudes at collapse point at load busbars. It is interesting to observe that, as expected, the voltage at bus #2 is characterized by the lowest amplitude being this bus the most loaded one (see values reported in Table I).

Case 2

The imposed lower and upper bounds for generators active and reactive powers and for the generator positive sequence voltage magnitudes in the OPF model solved at step *i*) are the same as in Case 1 (Table X).

As an example of the results obtainable at the end of the first step, Table XIV reports the mean values and the standard deviations of the voltage magnitude at the generator terminal busbar #6. A low value of standard deviation was experimented, mainly on the voltage amplitudes.

The mean value of voltage amplitude at the generator busbars does not reach the maximum value of 1.1 p.u., as in Case 1; this is mainly due to the binding of the upper bound (i.e., 1.1 p.u.) of the phase voltage amplitude at load bus #1.

Also in this case, the generator positive sequence voltage magnitude at busbar #6 assumes a value at the critical point lower than the specified voltage magnitude at the base operating point. In particular, at the critical point, the mean value of the generator positive sequence voltage magnitude is equal to 0.948 p.u. lower than 1.089 p.u. that is the mean value characterizing the base operating point (Table XIV).

Table XV reports the mean value and the standard deviation of the loading factor at the voltage collapse point. It is interesting to compare the results of Tabs. XV and XII (Case 2); in particular the probabilistic approach furnishes an expected value of the loading factor (i.e., $\mu(\lambda_{max})$= 0.904) greater than the value obtained in the deterministic approach (i.e., λ_{max} = 0.774).

In Fig 5 the pdf of the maximum loading factor is plotted; also in this case study the shape of the pdf approaches a Gaussian pdf with a value of the standard deviation very close to the value calculated in symmetrical case study (Case 1). In particular the value of standard deviation, in both cases, practically coincides with the values of 10% assigned to load powers.

Table XV reports the mean value of the phase voltage amplitude at collapse point at the load buses. The mean values of the voltage amplitudes of the three different phases are significantly unbalanced at the collapse point and, as foreseeable, the voltage of phase a is characterized by the lowest amplitude being this phase the most loaded one.

TABLE XIV - MEAN VALUE AND STANDARD DEVIATION OF POSITIVE SEQUENCE VOLTAGE MAGNITUDE AT GENERATOR BUSBARS #6 AT CRITICAL POINT - *FORMULATION C*

Case study	**Positive sequence voltage amplitude [p.u.]**	
	μ_V	σ_V
Case 1	1.100	0
Case 2	1.089	0.0021

TABLE XV - MEAN VALUE AND STANDARD DEVIATION OF THE LOADING FACTOR VALUES AT CRITICAL POINT - *FORMULATION C*

Maximum loading factor		
Case study	**Mean value**	**Standard deviation**
Case 1	1.153	9.36 %
Case 2	0.904	10.17 %

TABLE XVI - MEAN VALUE OF THE VOLTAGE AMPLITUDES AT LOAD BUSES AT CRITICAL POINT- *FORMULATION C*

	Mean values of phase voltage amplitudes [p.u.]			
Load Bus	**Case 1**	**Case 2**		
	Phases a, b and c	**Phase a**	**Phase b**	**Phase c**
#1	0.748	0.781	0.905	0.860
#2	0.723	0.777	0.906	0.857
#3	0.754	0.786	0.906	0.864

#4	0.835	0.880	0.952	0.936
#5	0.925	0.945	1.002	0.994

Case 3

As it is well known, the OPF can have different objective functions (e.g., the total production costs, system losses, etc…). To evaluate the sensitivity of the results with respect to the objective function minimized to determine the base operating point, a further case study was analysed. In particular, with respect to step *i* of the Formulations B and C, the problem was solved again with the base operating point obtained by the minimization of the total production costs.

For the production costs, quadratic unit cost functions ($C(P)=C_0+C_1 P+C_2 P^2$) were considered and the functions were characterized by the following parameters [5]:

- generator 1: C_0= 100 \$/h; C_1= 20 \$/MWh; C_2= 0.05 \$/(MW)^{2}h;
- generator 2: C_0= 200 \$/h; C_1= 25 \$/MWh; C_2= 0.10 \$/(MW)^{2}h.

The results obtained were very close to the ones obtained minimizing the power losses. This is due to different reasons; we just recall that, in the solution of the OPF, some bus voltage constraints are binding and force the solution.

For sake of brevity, only the pdfs of the maximum loading factor obtained by applying the Formulation C with the minimization of the cost production are reported. These pdfs, referred to the same study cases analysed applying the system power losses minimization, are illustrated in Figures 6 and 7. Comparing these pdfs with the ones shown in Figures 4 and 5 it clearly appears that the pdfs obtained with the minimization of power losses are slightly different to the pdfs obtained with the cost production minimization.

V. CONCLUSIONS

The voltage stability problem was considered for unbalanced three phase power systems and taking into account the problem of generator reactive power limits. New optimization models useful to quantify voltage stability limits in complex unbalanced power system were proposed. The reactive power limits were included in the optimization model using the complementarity constraints.

Different formulations, with increasing complexity, of the optimization model were proposed and tested. In particular, the maximum stability margin was calculated by a single-stage or a multi-stage procedure. In the latter case, to account for the relationship between the base operating point and the maximum loading point, a preliminary evaluation of the base operating point was conducted. In addition, the multi-stage maximum stability margin problem was formulated also in a probabilistic framework to account for the uncertainties affecting the input data, as the load powers. Numerical examples demonstrating the effectiveness of the proposed models under unbalanced operating conditions were provided.

The main conclusions of the paper are that: (i) generator reactive power limits can affect an unbalanced power system approaching the voltage collapse point; (ii) the complementarity constraints are a powerful tool to correctly represent synchronous machine behavior operating in unbalanced power systems approaching the voltage collapse point, (iii) the proposed probabilistic formulation permits to analyze the influence of the uncertainties affecting the power system operating conditions (e.g., active and reactive load powers) on the voltage stability limits.

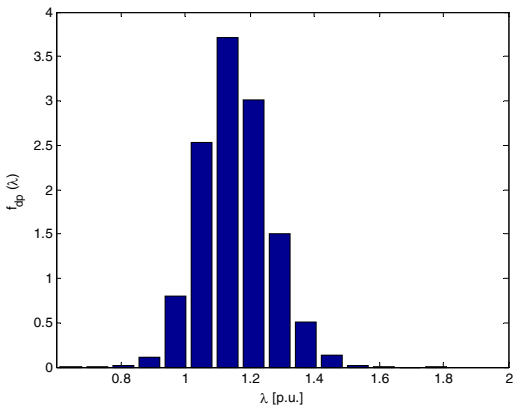

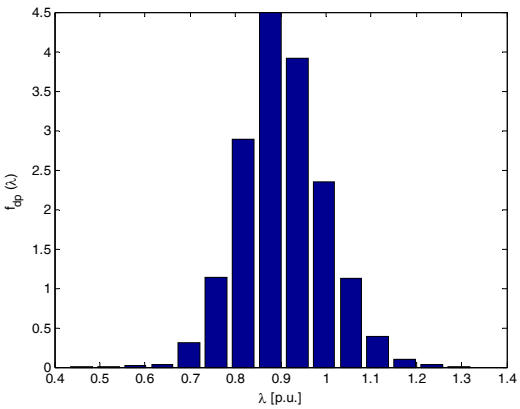

Fig. 4 - Probability density function of the maximum loading factor (*Formulation C* - Case 1).

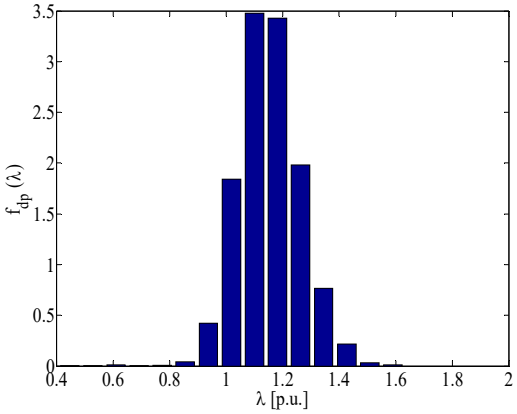

Fig. 5 - Probability density function of the maximum loading factor (*Formulation C* - Case 2)

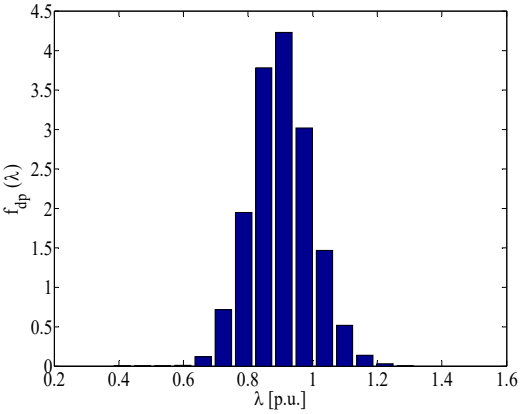

Fig. 6 - Probability density function of the maximum loading factor (*Formulation C* - Case 3).

Fig. 7 - Probability density function of the maximum loading factor (*Formulation C* - Case 3)

VI. REFERENCES

[1] T. Van Cutsem: "Voltage Instability: Phenomena, Countermeasures, and Analysis Methods", *Proc. IEEE*, Vol.88, n. 2, 2000, pp. 208-2227

[2] P. Kundur: "Power System Stability and Control", McGraw Hill, New York, USA, 1994

[3] R.J. Avalos, C.A. Canizares, F. Milano, A.J. Conejo: "Equivalency of Continuation and Optimization Methods to Determine Saddle-node and Limit-induced Bifurcations in Power Systems", *IEEE Trans. On Circuits and Syst*ems, Vol. 56, n. 1, 2009, pp. 210-222

[4] T. Niknam, M.R. Narimani, J. Aghaei, R. Azizipanah-Abarghooee, "Improved particle swarm optimisation for multi-objective optimal power flow considering the cost, loss, emission and voltage stability index," *IET Gener., Transm. & Distr.*, vol. 6, no. 6, pp. 515-527, June 2012

[5] A. Gomez Esposito, A.J. Conejo, C. Canizares: "Electric Energy Systems Analysis and Operation", Taylor & Francis Group, New Jork, 2009

[6] X.P. Zhang, P. Ju, E. Handschin: "Continuation Three-phase Power Flow: A Tool for Voltage Stability Analysis of Unbalanced Three-phase Power Systems", *IEEE Trans. Power Syst*., Vol.21, n. 3, 2005, pp. 1320-1329

[7] G. Carpinelli, D. Lauria, P. Varilone: "Voltage Stability Analysis in Unbalanced Power Systems by Optimal Power Flow", IEE Proc. Gen, Trans., Distrib., Vol. 153, n. 3, 2006, pp. 261-268

[8] M. Mamdouh Abdel-Akher, M.E. Ahmad, R.N. Mahanty,K.M. Nor: "An Approach to Determine a Pair of Power-Flow Solutions Related to the Voltage Stability of Unbalanced Three-Phase Networks", IEEE Trans. on Power systems, Vol. 23 , n. 3, 2008 , Pp 1249 –1257

[9] M. Abdel-Akher, "Voltage stability analysis of unbalanced distribution systems using backward/forward sweep load-flow analysis method with secant predictor," *IET Gener., Transm. & Distr.*, vol. 7, no. 3, pp. 309-317, March 2013

[10] F.M. Echavarren, E. Lobato, L. Rouco "Steady-state analysis of the effect of reactive generation limits in voltage stability" Electric Power Systems Research, Vol 79, 2009, pg. 1292–1299

[11] P. Caramia, G. Carpinelli, P.Varilone: "Voltage Stability Analysis in Unbalanced Three-phase Power Systems with Complementarity Constraints", Proceedings of 13th International Conference on Environment and Electrical Engineering (EEEIC'13),Wroclaw, Poland, 2013

[12] W. Rosehart, C. Roman, A. Schellemberg: "Optimal Power Flow with Complementarity Constraints", IEEE Trans. Power Syst., Vol. 20, n. 2, 2005, pp. 813-822

[13] J. Arrillaga, C.P. Harnold, B.J. Harker: "Computer Analysis of Power Systems", J. Wiley, USA, 1990

[14] B. Borkowska: "Probabilistic load Fow" IEEE Trans on Power Apparatus and Systems, Vol. 93, n.. 3, 1974, pp. 752-759.

[15] R.N. Allan, B. Borkowska, C.H. Grigg: "Probabilistic analysis of power Flows", IEE Proceedings, Vol. 121, n.. 12, 1974, pp. 1551-1556.

[16] M. Schilling, AM. Leite da Silva, R. Billington, MA. El-Kady: "Bibliography on power system probabilistic analysis", IEEE Trans on Power System, Vol. 5, No. 1, pp. 1-11, 1990.

[17] P. Caramia, G. Carpinelli, P. Varilone, P. Verde: " Probabilistic three-phase load flow", International Journal of Electrical Power& Energy Systems, vol. 21, 1996, p. 55-69.